Available online at www.sciencedirect.com
ScienceDirect
Journal of the European Ceramic Society 28 (2008) 1575–1583
www.elsevier.com/locate/jeurceramsoc

Optimal strength and toughness of Al_2O_3–ZrO_2 laminates designed with external or internal compressive layers

Raúl Bermejo *, Javier Pascual, Tanja Lube, Robert Danzer

Institut für Struktur- und Funktionskeramik, Montanuniversität Leoben, Peter-Tunner Straße 5, A-8700 Leoben, Austria

Received 25 July 2007; received in revised form 25 October 2007; accepted 2 November 2007
Available online 4 March 2008

Abstract

Layered ceramics have been proposed as an alternative choice for the design of structural ceramics with improved fracture toughness, strength and reliability. The use of residual compressive stresses, either at the surface or in the internal layers, may improve the strength as well as the crack resistance of the material during crack growth. In this work, two alumina–zirconia laminates designed with external (ECS-laminates) and internal (ICS-laminates) compressive stresses have been investigated using a fracture mechanics weight function analysis. An optimal architecture that maximises material toughness and strength has been found for each design as a function of geometry. From a flaw tolerant viewpoint, ECS-laminates are suitable for ceramic components with small cracks or flaws which are embedded in or near the potential tensile surface of the piece. On the other hand, the existence of large cracks or defects suggests the use of ICS-laminates to attain a more reliable response.

Keywords: Composites; Toughness and toughening; Strength; Al_2O_3–ZrO_2; Weight function

1. Introduction

The increased number of engineering design constraints, driven by the growing product requirements, as well as the greater range of advanced materials now available face the designer with complex choices for selecting a material to meet the performance of a particular system. The outcome of competition between various classes of materials is given not only by the combination of their intrinsic properties but also by the processing capability that they may offer for being tailored for specific tasks. The development and implementation of multilayered ceramics for structural applications is an excellent example of the above design and material selection approach.[1–4]

Layered ceramic composites have been proposed as an alternative design to enhance the strength reliability of ceramic components as well as to improve their fracture toughness by means of energy release mechanisms, such as crack deflection or crack bifurcation.[5–10] A direct consequence of these energy-dissipating toughening mechanisms, which reduce the crack driving force at the crack tip, is the development of an increasing crack growth resistance, i.e. R-curve behaviour. Ceramics that exhibit this behaviour can show not only reduced scatter in fracture strength (higher reliability) but also, in some cases, higher fracture loads compared to brittle materials with no crack-growth resistance. A commonly used multilayer design is that which combines layers with different densification during cooling from the sintering temperature, yielding as a result a tensile-compressive residual stress distribution in the laminate. The specific location of the compressive layers, either at the surface or internal, is associated with the attempted design approach, based on either mechanical resistance or damage tolerance, respectively. In the former case, the effect of the compressive residual stresses results in a higher, but single-value, apparent fracture toughness together with enhanced strength (the main goal) and some improved reliability.[11–13] On the other hand, in the latter case, the internal compressive layers are microstructurally designed to rather act as stopper of any potential processing and/or machining flaw at the surface layers, independent of original defect size (threshold strength), such that failure tends to take place under conditions of maximum crack growth resistance.[14–17] From this viewpoint, much effort has been put in the fabrication of laminates with a tailored residual stress profile arising from mismatch of elastic properties and thermal expansion coefficients between layers, selective phase

* Corresponding author. Tel.: +43 3842 402 4115; fax: +43 3842 402 4102.
E-mail address: raul.bermejo@mu-leoben.at (R. Bermejo).

0955-2219/$ – see front matter © 2007 Elsevier Ltd. All rights reserved.
doi:10.1016/j.jeurceramsoc.2007.11.003

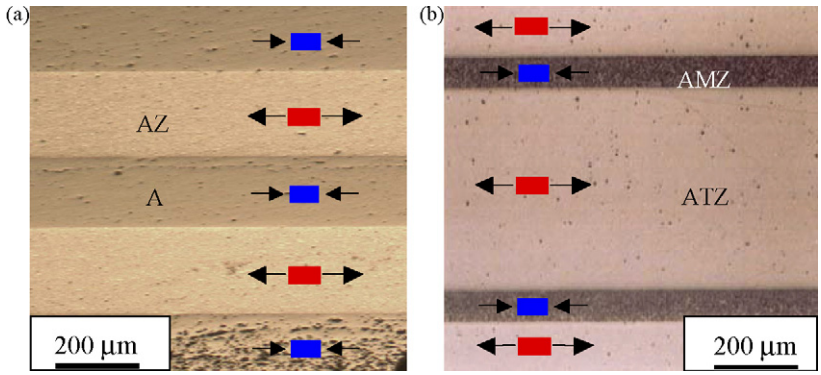

Fig. 1. Cross-section detail of the two alumina–zirconia layered architectures investigated, designed with (a) external compressive layers (ECS-laminates) and (b) internal compressive layers (ICS-laminates).

transformation and/or chemical reactions.[18–20] Within this context, alumina–zirconia layered systems have been extensively investigated as an alternative route for enhancing the mechanical response of alumina-based monolithic ceramics in terms of strength and/or fracture toughness.[19,21–26]

The aim of this work is to optimise the architectural design of ceramic multilayered systems as a function of its potential application. In doing so, two alumina–zirconia systems designed with external or internal compressive stresses respectively are compared using a fracture mechanics weight function analysis. An example of such layered architectures can be seen in Fig. 1, where tailored residual compressive stresses were introduced in the laminates during sintering, either in the surface layers or in the internal ones. The material designed with external compressive stresses, named ECS-laminate, consists of alternated tape cast sheets of alumina/stabilised-zirconia (AZ) composite and sheets of pure-alumina (A), following the sequence A/AZ/A, . . ., A/AZ/A.[27] The material fabricated with internal compressive stresses, referred to as ICS-laminate, is made of alumina/pure-zirconia (AMZ) layers sequentially slip cast with alumina/stabilised-zirconia (ATZ) layers as ATZ/AMZ/ATZ, . . ., ATZ/AMZ/ATZ.[28]

An optimal architecture that maximises both material toughness and strength is sought for each layered design as a function of its layer thickness ratio. The influence of elastic properties and number of layers is also discussed.

2. Experimental procedure

2.1. Laminates of study

In this work, symmetrical laminates fabricated with nine alternated layers and a fixed total thickness of $W = 3$ mm, according to a possible design condition, were studied. All the layers made of the same material (A, AZ, ATZ or AMZ, respectively) have the same thickness, so that the laminate is well defined by the number of layers, N, and the layer thickness ratio, $\lambda = t_{int}/t_{ext}$. The indexes "ext" and "int" refer to the external and first internal layer for each case. Table 1 summarises the material properties corresponding to the layers of both laminates, where the Young's modulus, E, and Poisson's ratio, ν, were measured by impulse excitation technique, the coefficient of thermal expansion, α, by means of a dilatometer between 20 and 1200 °C and the intrinsic toughness K_0 following the VAMAS procedure (single-edge-V-notch beam in four-point bending test).[29,30]

2.2. Residual stresses

As a result of the thermo-elastic mismatch between adjacent layers occurring during sintering, a uniform and biaxial residual stress distribution parallel to the layer plane appears in the laminate far away from the free surfaces (Fig. 1). For the case of ECS-laminates the thermal mismatch between layers is given by the different thermal expansion capability of the AZ layers with respect to the A layers, due to the zirconia content of the former. On the other hand for the ICS-laminates the significant thermal mismatch between adjacent layers is associated with the zirconia phase transformation occurring in the AMZ layers during cooling down from sintering.[28] The magnitude of these residual stresses can be assessed by[31]:

$$\sigma_{res,int} = -E'_{int}\frac{\int_{T_0}^{T_{sf}} \Delta\alpha \, dT}{[1 + (N-1)/(N+1)](e/\lambda)} \quad (1a)$$

$$\sigma_{res,ext} = -\sigma_{res,int}\frac{(N-1)}{(N+1)}\lambda \quad (1b)$$

where $E' = E/(1-\nu)$, ν being the Poisson's ratio, $\Delta\alpha = (\alpha_{ext} - \alpha_{int})$ is the difference of the thermal expansion coefficients between two adjacent layers, T_{sf} is the temperature below which the residual stresses arise (considered to be 1200 °C), T_0 is the room temperature, and $e = E'_{ext}/E'_{int}$.

It is known that the residual stress state associated with the above-mentioned parameters may condition the crack growth

Table 1
Material properties corresponding to the layers of both ECS- and ICS-laminates

Material	E (GPa)	ν	$\bar{\alpha}$ (10^{-6} K^{-1}) (20–1200 °C)	K_0 (MPa m$^{1/2}$)
A	391	0.24	8.64	3.8
AZ	305	0.26	9.24	4.3
ATZ	390	0.22	9.82	3.2
AMZ	280	0.22	8.02[a]	2.6

[a] The low thermal expansion coefficient value is due to the volume increase associated with the $t \rightarrow m$ zirconia phase transformation in the AMZ layers during cooling[28].

resistance of the multilayered system.[14–16,23,24] In this work, the layer thickness ratio (λ) will be the parameter of study. A fracture mechanics analysis will be performed to optimise the fracture response for each design.

2.3. Weight function analysis

The apparent fracture toughness of a laminate with a residual stress distribution can be calculated considering the equilibrium condition at the crack tip, i.e. crack propagation is possible if the stress intensity factor at the crack tip equals or exceeds the intrinsic material toughness, K_0. In the case of materials with residual stresses, the stress intensity factor at the crack tip as a function of the crack length, $K_{tip}(a)$, can be given as the externally applied stress intensity factor $K_{appl}(a)$ plus the contribution of the residual stresses $K_{res}(a)$:

$$K_{tip}(a) = K_{appl}(a) + K_{res}(a) \quad (2)$$

Thus, solving Eq. (2) for $K_{appl}(a)$, the crack propagation criterion is fulfilled when:

$$K_{appl}(a) \geq K_0 - K_{res}(a) = K_R(a) \quad (3)$$

The term $K_{res}(a)$ can be assessed by means of the weight function approach, which allows us to calculate the apparent toughness $K_R(a)$ for an edge crack[1] of length a for an arbitrary stress distribution acting normal to the prospective fracture path as[33]:

$$K_R(a) = K_0 - \int_0^a h(x,a)\sigma_{res}(x)\,dx \quad (4)$$

where K_0 is the intrinsic fracture toughness of each individual layer (given in Table 1), x is the distance along the crack length measured from the surface, a is the crack length, and $h(a,x)$ is the weight function, as developed by Fett[34] for an edge crack in a 3-point bend bar, commonly employed in the evaluation of the R-curve behaviour for multilayered systems. The corresponding weight function is given by

$$h(a,x) = \left(\frac{2}{\pi a}\right)^{1/2} \frac{1}{(1-x/a)^{1/2}(1-a/W)^{3/2}} \times \left[\left(1-\frac{a}{W}\right)^{3/2} + \sum A_{\nu\mu}\left(1-\frac{x}{a}\right)^{\nu+1}\left(\frac{a}{W}\right)^{\mu}\right] \quad (5)$$

where W is the specimen thickness, and the coefficients $A_{\nu\mu}$ and exponents ν and μ determined using the "boundary collocation method"[34] are listed in Table 2. We caution the reader about the fact that a weight function that applies to a homogeneous material (with constant elastic properties) has been here considered. This approximation may lead to an overestimation of the calculated apparent fracture toughness in the ATZ layers of the ICS-laminates and in the A layers of the ECS-laminates, owed to the lower stiffness of the adjacent AMZ and AZ layers, respectively.[35,36] In this regard, an alternative procedure has been proposed elsewhere,[37] to predict in a more accurate way the fracture toughness of multilayered ceramics whose layers have different elastic properties. Nevertheless, this level of accuracy is beyond the scope of this work.

Table 2
Weight function coefficients ($A_{\nu\mu}$) for a 3-point bend bar determined by the "boundary collocation method"[34]

	$\mu=0$	$\mu=1$	$\mu=2$	$\mu=3$	$\mu=4$
$\nu=0$	0.50	2.45	0.07	1.32	−3.07
$\nu=1$	0.54	−5.08	24.35	−32.72	18.12
$\nu=2$	−0.19	2.56	−12.64	19.76	−10.99

The apparent fracture toughness, $K_R(a)$, was calculated according to the procedure explained above, integrating Eq. (4) by means of analytical software Mathematica© V.5.1. The influence of the different residual stress states, given by the layer thickness ratio (λ), on the apparent fracture toughness of the laminates has been examined in detail aiming to obtain architectures which yield the maximum shielding effect. Within this context, a linear elastic fracture mechanics analysis based on experimental flexural tests has also been implemented in order to provide an optimal design combining toughness and strength. The results are expressed for both ECS and ICS layered systems.

3. Results and discussion

3.1. Layer thickness ratio for maximum shielding

Fig. 2 shows the apparent fracture toughness for different layer thickness ratios (λ) in the layered architectures designed with external (Fig. 2a) and internal (Fig. 2b) compressive layers, as a function of a crack length parameter $\hat{a}$, expressed as $Y\sqrt{a}$, with Y defined for an edge in a crack 3-point bend bar and given by[38]:

$$Y(\delta) = \left[\frac{1.99 - \delta(1-\delta)(2.15 - 3.93\delta + 2.7\delta^2)}{(1+2\delta)(1-\delta)^{3/2}}\right], \quad \delta = \frac{a}{W} \quad (6)$$

As it can be inferred from Eq. (1), the architectural parameter λ influences the residual stress field. Thus, the apparent fracture toughness is represented for different values of λ (until the crack length a being approximately half of the specimen thickness) in order to determine the geometry that provides the maximum shielding in both laminates.

As shown by previous authors the apparent toughness curves of multilayers show an oscillating behaviour.[12,24,39–41] For the laminates with external compressive residual stresses, ECS-laminates, the toughness increases in the external layers with increasing crack length and reaches a local maximum at the A/AZ interface, whereas it decreases in the tensile layers reaching a local minimum at the AZ/A interface. For the ICS-laminates toughness decreases within the external layer up to the

[1] In this paper, edge crack refers to a straight crack running from the tensile surface of the laminate normal to the layer plane. It should not be confused with edge cracking phenomena occurring in some laminates due to the residual stresses.[32]

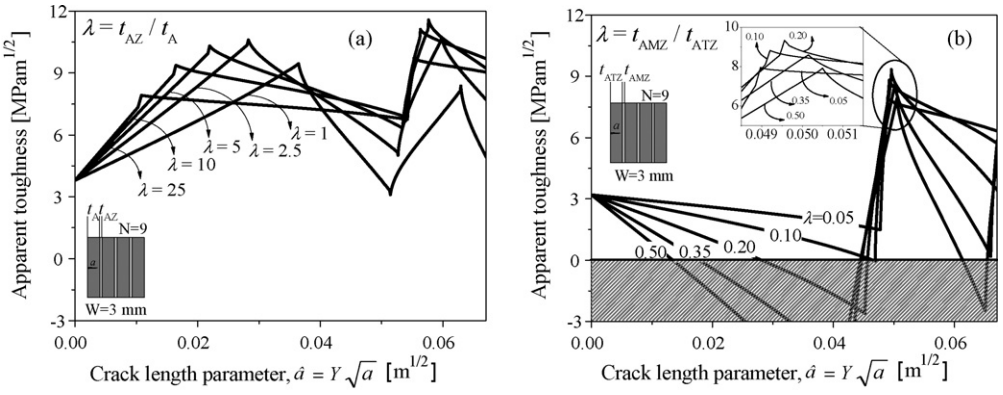

Fig. 2. Apparent toughness as a function of the layer thickness ratio (λ) in the layered architectures designed with (a) external and (b) internal compressive layers.

ATZ/AMZ interface, due to the negative contribution of the second term in Eq. (4) to the intrinsic fracture toughness of the ATZ layers. In some cases, the apparent fracture toughness of the laminate predicted by the weight function analysis may even result in negative values (see shaded area in Fig. 2b), owed to the significant tensile residual stresses in the thick ATZ layers. However, as soon as the crack enters the compressive AMZ layer, the apparent toughness rises up to a maximum value at the AMZ/ATZ interface. It can be stated that the compressive stresses shield the material against flaws, while the tensile stresses have a detrimental effect in the effective apparent toughness. Regarding the shielding effects as a function of the different geometries, i.e. various λ, the following aspects may be inferred from Fig. 2.

For the ECS-laminates λ is defined as t_{AZ}/t_A in the range of 1–25. Therefore, high values of λ correspond to thin A layers in comparison to the AZ layers, and thus high compressive stresses are present in the former according to Eq. (1). That is the reason why the shielding increases so steeply in the A layers and a high stress intensity factor should be applied to lead the specimen to failure (Fig. 2a). However, for low values of λ, the thickness of the A layers is much bigger than that of the AZ layers and as a result, high tensile stresses arise in these AZ layers. Hence, the effective toughness drops remarkably in the AZ layers for these laminates. An interesting conclusion drawn from Fig. 2a is the existence of an architecture that maximises the shielding at the first interface. Opposite to what could be expected, the highest surface compressive stress (the highest λ) does not correspond to the highest shielding in the first layer. Since the maximum shielding in the first layer is obtained at a distance equal to the outer layer thickness, the thickness t_A plays an important role. In this case, a maximum shielding factor at the first interface is achieved for geometries with a $\lambda_{max} \approx 2.5$, where a compromise between high compressive stresses and relative thick layer thickness applies, leading to an apparent toughness of ≈10.6 MPa m$^{1/2}$. In terms of layer thickness, this will correspond to A layers of $t_A \approx 200\,\mu m$ and AZ layers of $t_{AZ} \approx 500\,\mu m$. The residual stresses corresponding to this layered architecture can be calculated using Eq. (1), yielding compressive stresses of ≈−224 MPa in the A layers and tensile stresses of ≈+112 MPa in the AZ layers.

For the ICS-laminates λ is defined as t_{AMZ}/t_{ATZ} in the range of 0.05–0.5. Low λ values yield very thin AMZ layers with high compressive stresses and thick ATZ layers with negligible tensile stresses, as inferred from Eq. (1). On the other hand, relative high λ values lead to significant tensile residual stresses in the ATZ layers which may be detrimental for the material integrity. In any case, the shielding effect is provided by the internal AMZ compressive layers and, similar to the ECS-laminate design, an optimal apparent toughness (≈9.3 MPa m$^{1/2}$) is found for a geometry that combines high compressive stresses in the AMZ internal layers of a relative thick thickness. A maximal parameter of $\lambda_{max} \approx 0.2$ is found in such case, which would correspond to ATZ layers of $t_{ATZ} \approx 520\,\mu m$ and AMZ layers of $t_{AMZ} \approx 100\,\mu m$. The residual stresses associated with this layered architecture, calculated using Eq. (1), yield tensile stresses of ≈+109 MPa in the ATZ layers and compressive stresses of ≈−682 MPa in the AMZ layers. The fracture behaviour of this particular architecture has been experimentally assessed in.[17]

3.2. Residual stresses in the laminates of study

As explained above, the different residual stress state in the laminates is associated with the layer thickness ratio between layers (λ). Table 3 represents the magnitude of the biaxial residual stresses which develop in the layers of both ECS- and

Table 3
Magnitude of the biaxial residual stresses which develop in the layers of both ECS- and ICS-laminates for several geometries as a function of the layer thickness ratio (λ)

Ratio (λ)	Residual stress (MPa)			
	ECS-laminates		ICS-laminates	
	A	AZ	ATZ	AMZ
0.05	–	–	30	−740
0.10	–	–	57.5	−719
0.20	–	–	109	−682
0.35	–	–	177	−633
0.5	–	–	236	−591
1	−142	177	–	–
2.5	−224	112	–	–
5	−278	69	–	–
10	−315	39	–	–
20	−338	21	–	–
25	−343	17	–	–

ICS-laminates for several geometries. The values were calculated using Eq. (1), and the elastic and thermal properties were taken from Table 1.

The maximum shielding in both ECS- and ICS-laminates is given by an optimal combination of compressive stresses and layer thickness. However, the tensile residual stresses which balance the layered architecture must also be taken into account. In this case, however, the corresponding tensile stresses are about ≈100 MPa for both ECS- and ICS-laminates (see Table 3), which should not affect the integrity of the layered structure. This is an important factor to take into account, since a high tensile stress state could lead to the appearance of closed transverse cracks, so-called *tunnelling cracks*, which might negatively affect the material mechanical response.[42]

3.3. Implications of maximum shielding on strength

The weight function analysis performed above yields optimal design geometries in terms of maximum shielding for layered ceramics with tailored external/internal compressive stresses. In both cases, relative thick compressive layers are required to provide a maximum crack growth resistance for an edge crack under a tensile stress field. Due to the large variety of flaw sizes and population which may be encountered in a real ceramic component, flexural strength tests are often performed to identify both the shape and the kind of the critical defects causing the failure as well as their location within the specimen. It is well known that the failure stress variability of ceramic components often recalls the use of Weibull statistics to evaluate the strength of the material.[43–45] For some of the multilayered geometries here investigated, experimental four-point bending strength tests have been carried out in previous works, aiming to discern the type and size of critical flaws causing the material failure as well as to understand the fracture process of a crack propagating through the layered structure.[17,24,25,46]

Within the crack resistance context assessed in Section 3.1, a simple fracture mechanics analysis is here employed to better understand the implications of the maximum shielding provided by the layered geometries above described on the strength and fracture behaviour of both designs (ECS-laminates and ICS-laminates). In this regard, additionally to Eq. (3) which dictates the conditions for crack growth, a stable/unstable crack propagation criterion is given by the following equation, defined for each layer except at the interfaces:

$$\frac{dK_{appl}(a)}{da} \geq \frac{dK_{R,effective}(a)}{da} \quad (7)$$

when Eq. (7) is fulfilled, unstable crack propagation will occur. Whether or not the crack propagation yields to catastrophic failure will be associated with the capability of the layered structure to arrest the approaching crack.

3.3.1. ECS-laminates

Fig. 3 represents the crack growth resistance of several ECS-laminates (with different λ) as a function of the crack length parameter $\hat{a}$ in the region of maximum shielding. As reported in the previous sections, for the ECS-laminates, the maximum

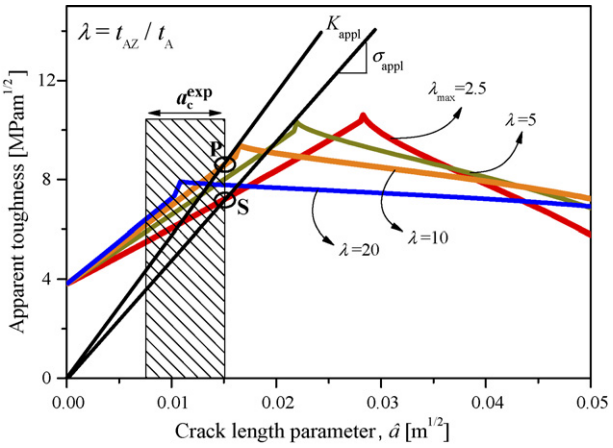

Fig. 3. Optimal apparent toughness and strength as a function of the layer thickness ratio (λ) in the layered architectures designed with external compressive layers. The range of flaw size experimental found (a_c^{exp}) is also represented.

shielding is achieved at the first A/AZ interface of the external compressive layer A, for a design corresponding to a layer thickness ratio of $\lambda_{max} = 2.5$. Experimental flexural tests carried out in some ECS-laminate geometries along with the corresponding inspection of the fracture specimens revealed a homogeneous surface defect population within the first A layer. Abnormally grown grains were identified as failure origins having a critical size of $a_c = 15–60\ \mu m$.[46] This flaw range is represented in Fig. 3 in terms of the crack length parameter $\hat{a}(0.0076–0.015\ m^{1/2})$, assuming the geometric factor Y given by Eq. (6). We caution the reader that other critical flaws such as embedded flaws or small semi-elliptical cracks may also be found in this type of laminates. Such defects are not as critical as the edge cracks here considered, which yields a certain overestimation of the critical parameter $\hat{a}$, namely, a safer design condition.

The straight lines in Fig. 3 represent a given applied stress intensity factor K_{appl} which increases linearly as the crack length parameter $\hat{a}$ rises, and whose slope corresponds to the applied stress σ_{appl}, according to the following equation:

$$K_{appl}(a) = \sigma_{appl} Y \sqrt{a} = \sigma_{appl} \hat{a} \quad (8)$$

When this line intersects the effective apparent toughness of the material (K_R), Eq. (3) is fulfilled and crack propagation occurs. In addition, if Eq. (7) is satisfied, the crack propagates in an unstable manner until it reaches a region were Eq. (7) may no longer apply. For the particular geometry of maximum shielding (λ = 2.5), and considering the largest critical flaw found experimentally ($\hat{a} \approx 0.015\ m^{1/2}$), the crack propagation will take place when the applied stress intensity factor K_{appl} overcomes the apparent toughness of the laminate according to Eq. (3), represented by point **S** in Fig. 3. Moreover, since Eq. (7) is also fulfilled at this point, crack propagation will be unstable leading to catastrophic failure. Hence, the slope of this line (representing the applied stress, σ_{appl}) can be considered as the failure stress of the laminate. An interesting observation can be inferred from Fig. 3 when estimating the failure stress corresponding to other geometries (such as λ = 10) for the same critical flaw size. Within this context, the applied stress intensity factor nec-

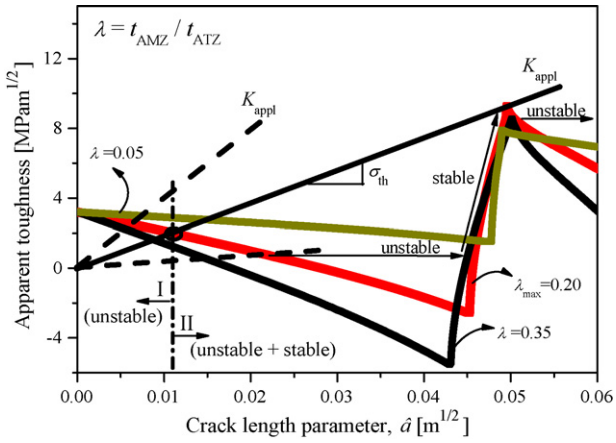

Fig. 4. Optimal apparent toughness and strength as a function of the layer thickness ratio (λ) in the layered architectures designed with internal compressive layers.

essary to satisfy Eq. (3) is now higher (point **P** in Fig. 3), as well as the corresponding applied stress (higher slope). Such design yields a maximum apparent toughness of ≈9.4 MPa m$^{1/2}$ which is almost 2.5 times that of the corresponding alumina monolith taken as a reference. Therefore, an optimal geometry ($\lambda = 10$) which combines maximal strength and high shielding is here proposed for the investigated ECS-laminates, now designed with external compressive layers (A) of $t_A \approx 66$ μm and internal tensile layers (AZ) of $t_{AZ} \approx 660$ μm. The corresponding residual stress state of this optimal layered architecture is listed in Table 3. The compressive stresses in the A layers are higher than those for the design of maximum shielding, which in fact contributes to higher values of strength. Moreover, the tensile stresses within the AZ layers are significantly smaller. This is beneficial with respect to avoiding other types of damages, e.g. tunnelling cracks, which may affect the structural integrity of the material.

3.3.2. ICS-laminates

Fig. 4 shows the crack growth resistance of several ICS-laminates (with different λ) as a function of the crack length parameter $\hat{a}$ in the region of maximum shielding. For the ICS-laminates, the maximum shielding is achieved at the AMZ/ATZ interface of the internal compressive layer (AMZ), with an optimal design given by a layer thickness ratio of $\lambda_{max} = 0.2$.

A similar approach analogous to the previous section has been attempted to establish the conditions for stable/unstable crack propagation. As it can be inferred from Fig. 4, a different situation to the ECS-laminates can be observed. In this case, the critical flaw size will determine whether the applied stress intensity factor leads to catastrophic failure. In this regard, two regions corresponding to unstable (region I) or to unstable/stable crack propagation events (region II) may be defined for each architecture (Fig. 4). For short cracks which fall within region I, the condition for crack propagation given by Eq. (3) will also imply unstable crack propagation, since Eq. (7) is also satisfied within the compressive AMZ layer. However, large cracks that are found in region II will experience an initial unstable growth up to a certain point within the compressive AMZ layer where Eq. (7) no longer applies (Fig. 4). A further applied stress will yield stable crack growth up to the point of maximum shielding, where Eq. (7) is again satisfied, and thus, unstable crack propagation will follow. In these cases (region II), failure occurs at a defined stress level (so-called threshold stress, σ_{th}) and a fixed critical crack size, regardless of the initial defect size. Experimental four-point bending tests performed in previous works for a particular design, i.e. $\lambda \approx 0.2$, showed in fact two trends in terms of failure stress levels.[24] On the one hand, when the failure was originated from natural flaws embedded near the surface, a failure stress level of 360 ± 14 MPa was achieved, associated with small critical defects of $a_c = 65 \pm 18$ μm (mostly agglomerates located near the surface in the ATZ layer).[24] In such cases, the corresponding critical stress intensity factor calculated using Eq. (8), assuming a Y factor for embedded flaws as $2/\pi$, resulted in 3.25 ± 0.1 MPa m$^{1/2}$, thus being the fracture process governed by the ATZ material. However, on the other hand, indentation-strength experiments (where large indentation cracks where introduced in the tensile ATZ surface) yielded a very constant although lower failure stress, i.e. 167 ± 4 MPa.[17] In such cases an initial crack growth of the indentation up to the ATZ/AMZ interface was observed, as predicted in Fig. 4. The corresponding critical stress intensity factor given by Eq. (8) assuming the critical flaw size as an edge crack of approximately the ATZ + AMZ layer thickness, results in ≈8.6 MPa m$^{1/2}$, which is in agreement with the maximum apparent toughness predicted in Fig. 4 for such geometry. Following these ideas, we can conclude that ICS-laminates with small flaws show similar mechanical strength as ATZ monoliths. However, for laminates containing large cracks a reliable design in terms of a minimum failure stress (threshold strength) is associated with the maximum shielding provided by the AMZ compressive layer (Fig. 4).

Overall, from a flaw tolerant viewpoint, laminates designed with compressive stresses in the outer layers (ECS-laminates) seem to be suitable for ceramic components with small cracks or flaws which are embedded in or near the potential tensile surface of the piece. In such a case, an optimal architectural design which combines high strength with a significant high toughness can be achieved using relatively thin external compressive layers, which contain the most critical flaw. On the other hand, the existence of large cracks or defects suggests the use of laminates designed with compressive stresses in the inner layers (ICS-laminates) in order to attain a more reliable response, being the maximum shielding provided by the internal compressive layers the key factor for structural design.

3.4. Influence of elastic properties and number of layers

The influence of the elastic mismatch between layers has been investigated by varying the Young's modulus of the internal layers for both ECS- and ICS-laminates. Fig. 5 represents the maximum apparent toughness associated with each layer geometry (λ) as a function of $e = E_{ext}/E_{int}$, for ECS- and ICS-laminates, respectively. It is shown how a stiffer material in the inner layers ($\uparrow E_{int}$) will increase the toughness in both ECS- and ICS-laminates. Another interesting conclusion drawn from this figure is that, for the case of laminates with external compressive

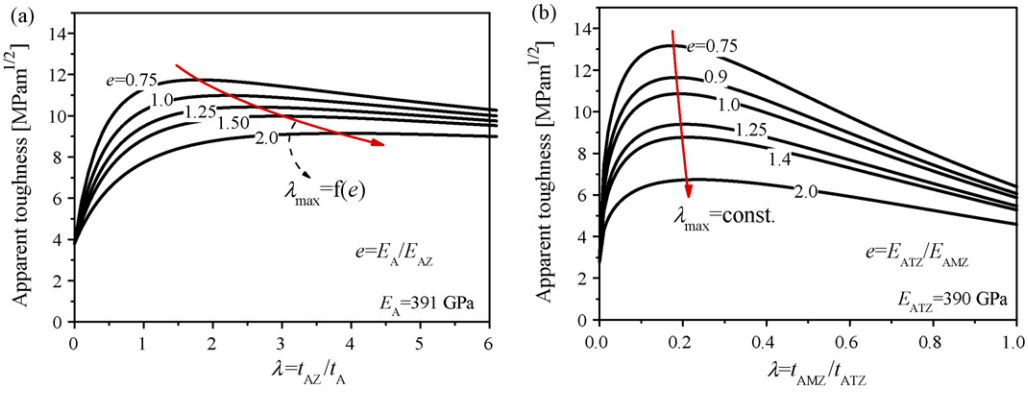

Fig. 5. Influence of the elastic mismatch between layers on the maximum shielding (λ_{max}) for (a) ECS-laminates and (b) ICS-laminates.

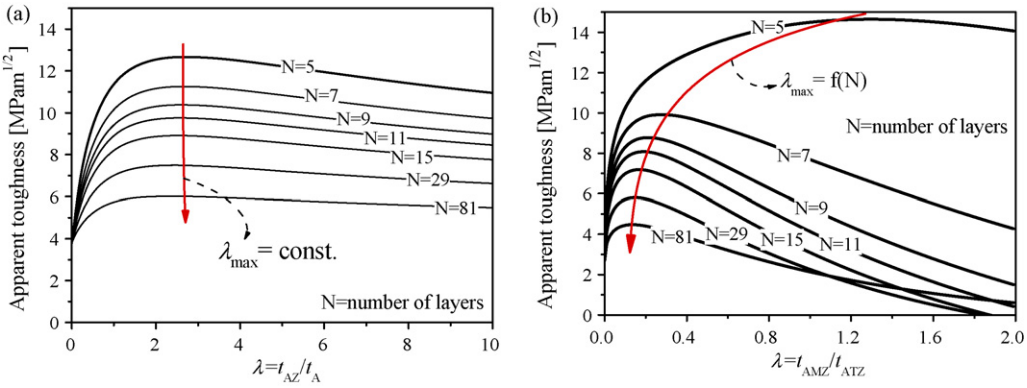

Fig. 6. Influence of the different number of layers (N) on the maximum shielding for (a) ECS-laminates and (b) ICS-laminates.

layers (ECS-laminates), the optimal layer thickness ratio (λ_{max}) in terms of maximum shielding increases for more compliant internal layers ($\downarrow E_{AZ}$), yielding as a result lower maximum apparent fracture toughness (Fig. 5a). However, for the case of ICS-laminates, the elastic properties of the internal layers have no significant effects on the optimal layer thickness ratio, leading to an almost constant λ_{max} value (Fig. 5b).

An additional study was performed to account for the influence of the different number of layers (N) on the shielding effects for both ECS- and ICS-laminates. As inferred from Eq. (1), N modifies the residual stress field thus influencing the crack growth resistance. The reader should keep in mind that for this work the stress field considered is given by Eq. (1), thus introducing some error in the outer layer since it does not consider the free surface effect on the residual stress distribution.[47] Using a finite element model developed elsewhere,[24,41] it has been observed that this discrepancy is not significant in most of the geometries here investigated. However, for laminates with relatively thick layers, i.e. $N \leq 5$, the model predicts a non-uniform residual stress field within the layers (Saint-Venant's principle) and the constant residual stress distribution here considered would not apply. As it can be inferred from Fig. 6a, the different number of layers in the ECS-laminate architecture does not influence the position of the maximum shielding, given for a layer thickness ratio of $\lambda_{max} \approx 2.5$. Under these conditions, a maximum apparent toughness value of $\approx$12.5 MPa m$^{1/2}$ might be achieved at the A/AZ interface for $N = 5$. On the other hand, for the case of ICS-laminates (Fig. 6b), the optimal thickness ratio is found to slightly increase as the number of layers diminishes. An interesting feature is found for architectures with 5 layers, where the λ_{max} results in 1.3, i.e. compressive AMZ layers thicker than the ATZ ones. In such a case, a maximum shielding level up to $\approx$14 MPa m$^{1/2}$ might be tailored at the AMZ/ATZ interface.

Following these ideas, both elastic properties and number of layers should also be taken into account for optimal reliable design, according to processing capabilities and final performance of the component.

4. Conclusions

In this work, two alumina–zirconia geometries designed with external (ECS) and internal (ICS) compressive layers have been investigated using a fracture mechanics weight function analysis. In general, ECS-laminates maximise their apparent toughness at the first interlayer (A/AZ), for a relative thin outer compressive (A) layer. On the other hand, ICS-laminates reach the maximum apparent toughness at the second interface (AMZ/ATZ) for architectures containing a relative thick tensile outer (ATZ) layer. In terms of strength, an optimal design has been found based on experimental results considering laminates of 9 layers and a total thickness of 3 mm according to possible design conditions. A geometry which combines high strength and relative maximal shielding is here proposed for the ECS-laminates designed with A layers of $t_A \approx 66$ μm and AZ

layers of $t_{AZ} \approx 660\,\mu m$. Likewise, a reliable design in terms of maximum threshold strength and maximum shielding for the ICS-laminates would correspond to ATZ layers of $\approx 520\,\mu m$ and AMZ layers of $\approx 100\,\mu m$.

The variation of the elastic properties through the layered architecture shows how a stiffer material in the internal layers ($\uparrow E_{int}$) would increase the apparent toughness in both ECS- and ICS-laminates. In the former, the optimal layer thickness ratio ($\lambda = t_{AZ}/t_A$) that maximises shielding decreases for stiffer internal layers ($\uparrow E_{AZ}$). However, for the latter, the elastic mismatch between layers has no significant effects on the optimal layer thickness ratio ($\lambda = t_{AMZ}/t_{ATZ}$), yielding an almost constant value and thus a less restrictive design condition. Additionally, a modification of the geometry by reducing the number of layers (N) yields an increase in the maximum shielding capability for both laminates. While an optimal layer thickness ratio remains constant with N for the ECS-laminates, a tendency to increase was appreciated for the ICS-laminates, especially for architectures designed with few layers ($N \leq 5$).

From a flaw tolerant viewpoint, ECS-laminates seem to be suitable for ceramic components with small cracks or flaws which are embedded in or near the potential tensile surface of the piece. On the other hand, the existence of large cracks or defects suggests the use of ICS-laminates to attain a more reliable response, being the maximum shielding the key parameter design.

Acknowledgements

The authors express their gratitude to the ISTEC Faenza and ICV-CSIC Madrid for the elaboration of the specimens using in the experimental tests. Special thanks to Prof. Roger Morrell for the revision of the manuscript.

References

1. Schwartz, B. and Wilcox, D. L., Laminated ceramics. *Ceram. Age.*, 1967, **83**, 40–44.
2. Mistler, R. E., High strength alumina substrates produced by a multiple layer casting technique. *Am. Ceram. Soc. Bull.*, 1973, **52**, 850–854.
3. Clegg, W. J., Kendall, K., Alford, N. M., Button, T. W. and Birchall, J. D., A simple way to make tough ceramics. *Nature*, 1990, **347**, 455–457.
4. Chan, H. M., Layered ceramics: processing and mechanical behavior. *Annu. Rev. Mater. Sci.*, 1997, **27**, 249–282.
5. He, M. Y. and Hutchinson, J. W., Crack deflection at an interface between dissimilar elastic materials. *Int. J. Solids Struct.*, 1989, **25**, 1053–1067.
6. Phillipps, A. J., Clegg, W. J. and Clyne, T. W., Fracture-behavior of ceramic laminates in bending. Part 1. Modeling of crack-propagation. *Acta Metall. Mater.*, 1993, **41**, 805–817.
7. Oechsner, M., Hillman, C. and Lange, F., Crack bifurcation in laminar ceramic composites. *J. Am. Ceram. Soc.*, 1996, **79**, 1834–1838.
8. Sanchez-Herencia, A. J., James, L. and Lange, F. F., Bifurcation in alumina plates produced by a phase transformation in central, alumina/zirconia thin layers. *J. Eur. Ceram. Soc.*, 2000, **20**, 1297–1300.
9. Lugovy, M., Orlovskaya, N., Slyunyayev, V., Gogotsi, G., Kübler, J. and Sanchez-Herencia, A. J., Crack bifurcation features in laminar specimens with fixed total thickness. *Comp. Sci. Technol.*, 2002, **62**, 819–830.
10. Pontin, M. G. and Lange, F. F., Crack bifurcation at the surface of laminar ceramics that exhibit a threshold strength. *J. Am. Ceram. Soc.*, 2005, **88**, 1315–1317.
11. Hansen, J. J., Cutler, R. A., Shetty, D. K. and Virkar, A. V., Indentation fracture response and damage resistance of Al_2O_3–ZrO_2 composites strengthened by transformation-induced residual stresses. *J. Am. Ceram. Soc.*, 1988, **71**, C501–C505.
12. Lakshminarayanan, R., Shetty, D. K. and Cutler, R. A., Toughening of layered ceramic composites with residual surface compression. *J. Am. Ceram. Soc.*, 1996, **79**, 79–87.
13. Green, D. J., Tandon, R. and Sglavo, V. M., Crack arrest and multiple cracking in glass through the use of designed residual stress profiles. *Science*, 1999, **283**, 1295–1297.
14. Rao, M., Sanchez-Herencia, J., Beltz, G., McMeeking, R. M. and Lange, F., Laminar ceramics that exhibit a threshold strength. *Science*, 1999, **286**, 102–105.
15. Lugovy, M., Slyunyayev, V., Subbotin, V., Orlovskaya, N. and Gogotsi, G., Crack arrest in Si_3N_4-based layered composites with residual stress. *Comp. Sci. Technol.*, 2004, **64**, 1947–1957.
16. Sglavo, V. M., Paternoster, M. and Bertoldi, M., Tailored residual stresses in high reliability alumina-mullite ceramic laminates. *J. Am. Ceram. Soc.*, 2005, **88**, 2826–2832.
17. Bermejo, R., Torres, Y., Baudin, C., Sánchez-Herencia, A. J., Pascual, J., Anglada, M. *et al.*, Threshold strength evaluation on an Al_2O_3–ZrO_2 multilayered system. *J. Eur. Ceram. Soc.*, 2007, **27**, 1443–1448.
18. Green, D. J., Cai, P. and Messing, G. L., Residual stresses in alumina–zirconia laminates. *J. Eur. Ceram. Soc.*, 1999, **19**, 1517–2511.
19. Sanchez-Herencia, J., Moya, J. and Tomsia, A., Microstructural design in alumina–alumina/zirconia layered composites. *Scripta Mater.*, 1998, **38**, 1–5.
20. Krishnamurthy, R. and Sheldon, B. W., Stresses due to oxygen potential gradients in non-stoichiometric oxides. *Acta Mater.*, 2004, **52**, 1807–1822.
21. Cutler, R. A., Bright, J. D., Virkar, A. V. and Shetty, D. K., Strength improvement in transformation-toughened alumina by selective phase-transformation. *J. Am. Ceram. Soc.*, 1987, **70**, 714–718.
22. Moon, R. J., Bowman, K. J., Trumble, K. P. and Rödel, J., Fracture resistance curve behavior of multilayered alumina–zirconia composites produced by centrifugation. *Acta Mater.*, 2001, **49**, 995–1003.
23. Toschi, F., Melandri, C., Pinasco, P., Roncari, E., Guicciardi, S. and de Portu, G., Influence of residual stresses on the wear behavior of alumina/alumina–zirconia laminated composites. *J. Am. Ceram. Soc.*, 2003, **86**, 1547–1553.
24. Bermejo, R., Torres, Y., Sanchez-Herencia, A. J., Baudín, C., Anglada, M. and Llanes, L., Residual stresses, strength and toughness of laminates with different layer thickness ratios. *Acta Mater.*, 2006, **54**, 4745–4757.
25. Lube, T., Pascual, J., Chalvet, F. and De Portu, G., Effective fracture toughness in Al_2O_3–Al_2O_3/ZrO_2 laminates. *J. Eur. Ceram. Soc.*, 2007, **27**, 1449–1453.
26. Ambrozic, M. and Kosmac, T., Optimization of the bend strength of flat-layered alumina–zirconia composites. *J. Am. Ceram. Soc.*, 2007, **90**, 1545–1550.
27. Tarlazzi, A., Roncari, E., Pinasco, P., Guicciardi, S., Melandri, C. and de Portu, G., Tribological behaviour of Al_2O_3/ZrO_2–ZrO_2 laminated composites. *Wear*, 2000, **24**, 29–40.
28. Bermejo, R., Baudín, C., Moreno, R., Llanes, L. and Sánchez-Herencia, A. J., Processing optimisation and fracture behaviour of layered ceramic composites with highly compressive layers. *Comp. Sci. Technol.*, 2007, **67**, 1930–1938.
29. Damani, R., Gstrein, R. and Danzer, R., Critical notch root radius in SENB-s fracture toughness testing. *J. Eur. Ceram. Soc.*, 1996, **16**, 695–702.
30. Kübler, J., Procedure for determining the fracture toughness of ceramics using the single-edge-v-notched beam (SEVNB) method. In *ESIS Procedures and Documents. EMPA, Swiss Federal Laboratories for Materials Testing and Research*, ed. K.-H. Schwalbe. Dübendorf, Switzerland, 2000, p. 16.
31. Oel, H. J. and Fréchette, V. D., Stress distribution in multiphase systems. Part I. Composites with planar interfaces. *J. Am. Ceram. Soc.*, 1967, **50**, 542–549.
32. Ho, S., Hillman, C., Lange, F. F. and Suo, Z., Surface cracking in layers under biaxial, residual compressive stress. *J. Am. Ceram. Soc.*, 1995, **78**, 2353–2359.

33. Bueckner, A novel principle for the computation of stress intensity factors. *ZAMM*, 1970, **50**, 529–546.
34. Fett, T., Stress intensity factors and weight functions for the edge cracked plate calculated by the boundary collocation method, KfK-Report 4791. *Kernforschungszentrum Karlsruhe, Karlsruhe*., 1990, pp. 55.
35. Fett, T., Munz, D. and Yang, Y. Y., Direct adjustment procedure for weight functions of graded materials. *Fatig. Fract. Eng. Mater. Struct.*, 2000, **23**, 191–198.
36. Fett, T., Munz, D. and Yang, Y. Y., Applicability of the extended petroski-achenbach weight function procedure to graded materials. *Eng. Fract. Mech.*, 2000, **65**, 393–403.
37. Chen, C. R., Pascual, J., Fischer, F. D., Kolednik, O. and Danzer, R., Prediction of the fracture toughness of a ceramic multilayer composite—modelling and experiments. *Acta Mater.*, 2007, **55**, 409–421.
38. Strawley, J. E., Wide range stress intensity factor extressions for astm e399 standard fracture toughness specimens. *Int. J. Fract.*, 1976, **12**, 475–476.
39. Moon, R. J., Hoffman, M., Hilden, J., Bowman, K. J., Trumble, K. P. and Rödel, J., Weight function analysis on the r-curve behavior of multilayered alumina–zirconia composites. *J. Am. Ceram. Soc.*, 2002, **85**, 1505–1511.
40. Lugovy, M., Slyunyayev, V., Orlovskaya, N., Blugan, G., Kuebler, J. and Lewis, M., Apparent fracture toughness of Si_3N_4-based laminates with residual compressive or tensile stresses in surface layers. *Acta Mater.*, 2005, **53**, 289–296.
41. Pascual, J., Chalvet, F., Lube, T. and De Portu, G., R-curves in Al_2O_3–Al_2O_3/ZrO_2 laminates. *Key Eng. Mater.*, 2005, **290**, 214–221.
42. Bermejo, R., Sanchez-Herencia, A. J., Baudín, C. and Llanes, L., Tensiones residuales en cerámicas multicapa de Al_2O_3–ZrO_2: naturaleza, evaluación y consecuencias sobre la integridad estructural. *Bol. Soc. Esp. Ceram. V*, 2006, **45**, 352–357.
43. Danzer, R., A general strength distribution function for brittle materials. *J. Eur. Ceram. Soc.*, 1992, **10**, 461–472.
44. Danzer, R. and Lube, T., New fracture statistics for brittle materials. In *Fracture Mechanics of Ceramics, vol. 11*, ed. R. C. Bradt, D. P. H. Hasselmann, D. Munz, M. Sakai and V. Y. Shevchenkov. Plenum Publishing Corp., New York, 1996, pp. 425–439.
45. Danzer, R., Some notes on the correlation between fracture and defect statistics: are weibull statistics valid for very small specimens? *J. Eur. Ceram. Soc.*, 2006, **26**, 3043–3049.
46. Pascual, J., Chalvet, F., Lube, T. and De Portu, G., Strength distributions of ceramic laminates. *Mater. Sci. Forum*, 2005, **492–493**, 581–586.
47. Sergo, V., Lipkin, D. M., de Portu, G. and Clarke, D. R., Edge stresses in alumina/zirconia laminates. *J. Am. Ceram. Soc.*, 1997, **80**, 1633–1638.